

## References

- BLOW, D. M. & CRICK, F. H. C. (1959). *Acta Cryst.* **12**, 794–802.  
 BRITTON, D. (1972). *Acta Cryst.* **A28**, 296–297.  
 FISHER, R. G. & SWEET, R. M. (1980). *Acta Cryst.* **A36**, 755–760.  
 GRAINGER, C. T. (1969). *Acta Cryst.* **A25**, 427–434.  
 HENDRICKSON, W. A. & LATTMAN, E. E. (1970). *Acta Cryst.* **B26**, 136–143.  
 MURRAY-RUST, P. (1973). *Acta Cryst.* **B29**, 2559–2566.  
 RAMACHANDRAN, G. N. & SRINIVASAN, R. (1970). *Fourier Methods in Crystallography*. New York: Wiley.  
 REES, D. C. (1982). *Acta Cryst.* **A38**, 201–207.  
 REES, D. C. & LIPSCOMB, W. N. (1982). *J. Mol. Biol.* **160**, 475–498.  
 STUBBS, G. J. & DIAMOND, R. (1975). *Acta Cryst.* **A31**, 709–718.

*Acta Cryst.* (1987). **A43**, 36–42

### (3+1)-Dimensional Patterson and Fourier Methods for the Determination of One-Dimensionally Modulated Structures

BY W. STEURER

*Institut für Kristallographie und Mineralogie der Universität, Theresienstrasse 41, D-8000 München 2, Federal Republic of Germany*

(Received 15 July 1985; accepted 12 May 1986)

#### Abstract

Patterson and Fourier methods applied to one-dimensionally modulated structures in the (3+1)-dimensional space  $R_{3+1}$  can be very helpful tools for the calculation of starting parameters of the atomic modulation functions. The characteristics of the (3+1)-dimensional Patterson function [(3+1)-PF] are discussed for some typical modulation waves from a geometrical point of view as well as with the aid of known modulated phases. The influence of series termination errors, resulting from incomplete data sets, is demonstrated. The (3+1)-PF, in any case, yields sufficient basic information even if first-order satellites only are accessible. Of course, it is necessary to include higher orders if one wants to learn something about the shape of the modulation wave. A comparison is made with the Patterson methods used for the solution of modulated structures until now, and it is shown that they are special cases of the (3+1)-PF. Some applications are given for Fourier methods in  $R_{3+1}$ , for example, to detect fluctuations of the phase or the amplitude of the modulation wave.

#### 1. Introduction

In recent years an increasing number of commensurately and incommensurately modulated structures has been determined. In general the solution of the average structure presents no difficulties, but it can be problematical to find workable starting parameters for the refinement of the atomic modulation functions. Direct methods are available for superstructures (*cf. e.g.* Böhme, 1982) but there is no incommensurately modulated structure known to the author which has been solved using them, and the usual

Patterson methods are hardly interpretable for more complicated cases. Consequently, most of the modulated structures have been solved based on model considerations or in a rather straightforward way (*cf. e.g.* Horst, Tagai, Korekawa & Jagodzinski, 1981; Yamamoto, Nakazawa, Kitamura & Morimoto, 1984; Steurer & Adlhart, 1983*a, b*). However, there have been many attempts to apply Patterson techniques to get information independent of models. The most frequently used way is to describe the incommensurate modulation in a commensurate supercell, approximately, and to calculate the 'partial' or 'difference' Patterson synthesis using the superstructure reflections alone (*cf. e.g.* Frueh, 1953; Takéuchi, 1972; Böhm, 1978; Tomeoka & Ohmasa, 1982). As a result the Patterson map of the 'complementary' structure, the difference between the real modulated structure and the average structure, is obtained.

Another method has been derived by Toman & Frueh (1973*a, b*) by calculating the Patterson synthesis in the subcell using 'one set' of satellite reflections. The 'plus and minus' difference Patterson function (McConnell & Heine, 1984) is a similar approach and has been used primarily to obtain symmetry information. A detailed discussion of all these methods will be given in § 5 of this paper. The purpose of this study is to discuss the properties of the (3+1)-PF for some fundamental modulation functions and to give an aid to the application of this method in practical structure determination. For the sake of a clear representation plane modulation waves with equal amplitudes are investigated in the first place, but the (3+1)-PF is interpretable in more general cases as well. Naturally, in the case of asymmetric functions of very different shape the definition of a phase relation between two modulation waves will

become dubious and the (3+1)-PF can give information about amplitude sums or differences only. In the following, we will deal with sinusoidal modulation which can be used as a first approximation to all modulation functions, and with rectangular and triangular functions for the description of microdomain structures or cases of microtwinning.

## 2. The (3+1)-dimensional Patterson function

According to the superspace theory of de Wolff (1974), one-dimensionally modulated structures can be described in a fictitious (3+1)-dimensional lattice  $R_{3+1}$ . By this means the translational symmetry in the direction of the propagation of the modulation wave, lost in the three-dimensional space  $R_3$ , is restored. The (3+1)-dimensional elementary cell contains the atoms as continuous strings in the extra dimension. The actual state of the atoms in a particular cell of the crystal then corresponds to a section in  $R_{3+1}$ .

The Fourier transform of the intensities at the reciprocal-lattice points  $\mathbf{H} = h\mathbf{a}^* + k\mathbf{b}^* + l\mathbf{c}^* + m\mathbf{q}$  with the satellite vector  $\mathbf{q} = \alpha\mathbf{a}^* + \beta\mathbf{b}^* + \gamma\mathbf{c}^*$  ( $h, k, l, m$  integer,  $\alpha, \beta, \gamma$  at least one irrational and  $<1$ ) can be written in analogy to the three-dimensional expression (cf. *International Tables for X-ray Crystallography*, 1959)

$$P(UVWT) = 1/V_c \sum_h \sum_k \sum_l \sum_m I_{hklm} \times \cos 2\pi(hU + kV + lW + mT) \quad (2.1)$$

and equals the function

$$P(UVWT) = V_c \int_0^1 \int_0^1 \int_0^1 \rho(xyzt) \times \rho(x+U, y+V, z+W, t+T) dx dy dz dt \quad (2.2)$$

[ $V_c$  is the volume of the fundamental cell in  $R_3$  and  $\rho(xyzt)$  is the electron density in  $R_{3+1}$  (Yamamoto, 1982)]. The (3+1)-PF represents the vector function between the string-like atoms ('string atoms') of the (3+1)-dimensional elementary cell. It is centrosymmetric and a continuous function in the extra dimension. If the (3+1)-PF is projected on  $T$  the Patterson map of the average structure is obtained. Therefore, if the Patterson map of the average structure shows well resolved peaks for a particular interaction it might be promising to investigate the (3+1)-PF around this region. In the following, the (3+1)-PF of such a single 'string atom'-'string atom' interaction will always be discussed.

Fig. 1 shows the (1+1)-dimensional cell with two 'string atoms' generated by a symmetric rectangular displacive modulation of a one-dimensional structure with two point atoms at  $x_1$  and  $x_2$ . The electron density

in the cell is given by

$$\rho_1(xt) = \begin{cases} 1 & \text{for } x = x_1 + A \quad 0 < t < \frac{1}{2} \\ & x = x_1 - A \quad \frac{1}{2} < t < 1 \\ 0 & \text{otherwise} \end{cases} \quad (2.3)$$

and the analogous expression for the atom at  $x_2$ .

$P(UT)$  consists of three triangular functions of  $T$  at the positions  $U_1 = (x_2 - x_1) + 2A$ ,  $U_2 = (x_2 - x_1)$  and  $U_3 = (x_2 - x_1) - 2A$  as can be calculated using (2.2) or is easily derived from the picture. The magnitude of  $P(UT)$  is proportional to the sum over all equivalent vectors between the 'string atoms' with a particular  $T = \Delta t$  (compare the areas  $F_1$  and  $F_2$  in Fig. 1, for example). If the 'string atoms' are shifted by  $T = \Delta t$  against each other then the maximum area and therewith the maximum peak of  $P(UT)$  is obtained for the vector set with  $T = \Delta t$ . Thus, from the position of the 'bordering' peaks at  $U_1$  and  $U_3$  one can calculate the amplitude  $A$  and from the value of  $T$  of the maximum peak the phase difference can be derived.

Generally it can be said, and this is valid for all possible displacive and substitutional modulations, that the (3+1)-PF for an interaction between two 'string atoms' differing in phase only has its absolute maximum at  $\mathbf{R} = \Delta\mathbf{r}_{kk'}$  ( $\mathbf{R}$  is the vector with the components  $U, V, W$  and  $\Delta\mathbf{r}_{kk'}$  the vector between the atoms  $k, k'$  of the basic structure) and  $T = \Delta\varphi_{kk'}$  ( $\Delta\varphi_{kk'}$  is the phase difference between the modulation functions of the atoms  $k, k'$ ). In the case of displacive modulation the 'bordering' peaks (i.e. the vectors with the largest and smallest  $|\mathbf{R}|$ ) are at  $\mathbf{R} = \Delta\mathbf{r}_{kk'} \pm (\mathbf{A}_k + \mathbf{A}_{k'})$  ( $\mathbf{A}_k$  is the amplitude of the modulation wave of the atom  $k$ ) and  $T = \Delta\varphi_{kk'} + \pi$ . These peaks can be found, e.g. at  $U = \pm 0.1a$  and  $T = 0.5$  in Figs. 2(b) and 2(c). Consequently, from the position of the absolute maximum of the (3+1)-PF of a single interaction one can derive the phase difference  $\Delta\varphi_{kk'}$  and from the position of the 'bordering' peaks the sum of the amplitudes ( $\mathbf{A}_k + \mathbf{A}_{k'}$ ).

A more complicated Patterson map is obtained in the case of displacive modulation waves of the same shape but very different amplitudes (for practical cases differing at least by a factor two, considering average resolution). Then the position of the absolute

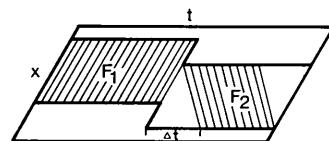


Fig. 1. A schematic representation of a (1+1)-dimensional elementary cell containing two rectangularly modulated point atoms as continuous strings in the extra dimension  $t$ . The number of equivalent vectors between the 'string atoms' with a particular  $T = \Delta t$  is proportional to the hatched areas  $F_1$  ( $T=0$ ) and  $F_2$  ( $T = \Delta t$ ), for example.

maximum of the (3+1)-PF of an interaction of two non-rectangular 'string atoms' need no longer be a correct measure for  $\Delta\varphi_{kk'}$ . The phase difference has to be derived from the position of the 'bordering' peaks at  $\mathbf{R} = \Delta\mathbf{r}_{kk'} \pm (\mathbf{A}_k + \mathbf{A}_{k'})$  which are for non-rectangular displacive waves at  $T = \Delta\varphi_{kk'} + \pi$  in any case.

Conversely, we can conclude that if we do not find the absolute maximum at  $\mathbf{R} = \Delta\mathbf{r}_{kk'}$ , which is known from the average structure, then the 'string atoms' involved have very different amplitudes  $\mathbf{A}_k, \mathbf{A}_{k'}$ . In the extreme case with one amplitude equal to zero a (3+1)-PF independent of  $T$  is obtained and only a rough estimate of the amplitude may be possible.

In order to avoid the evaluation of the (3+1)-PF in the complicated cases mentioned above, it may be advisable to calculate the (3+1)-PF for interactions of atoms being symmetrically equivalent preferably in  $R_{3+1}$ . This will be possible in all superspace groups but  $P^{p1}(\alpha\beta\gamma)$  and reduces the problem to the case of 'string atoms' with equal amplitudes and shape (at least for the first harmonic), allowing the determination of the amplitude. If there is a symmetry element in the superspace group turning  $\mathbf{q}$  into  $-\mathbf{q}$  then the phase  $\varphi_{k'}$  of the modulation function of the atom  $k'$ , generated by this symmetry operation from the function of the atom  $k$  with the phase  $\varphi_k$ , will be equal to  $-\varphi_k$  and  $\Delta\varphi_{kk'} = 2\varphi_k$ . The phase  $\varphi_k$  can be determined from this with an uncertainty of  $\pi$ . Hence, if one uses the (3+1)-PF in this way one obtains the simply evaluable maps, in principle, shown in Fig. 2.

Fig. 2(a) illustrates the case of an asymmetrically rectangularly modulated structure. The (3+1)-PF is a trapezoidal function of  $T$ . The width of the plateau parallel to the  $UT$  plane is proportional to the degree of asymmetry of the modulation function and becomes zero for symmetric rectangular waves. The Patterson maps for sinusoidal and triangular displacive modulation are given in Figs. 2(b) and 2(c). The maps look very similar and might not be distinguishable in practice.

Quite a different picture is obtained for the (3+1)-PF of sinusoidal substitutional modulation (Fig. 2d). The ratio of the maximum to the minimum of  $P(UVWT)$  is a measure of the amplitudes of the modulation functions involved. In the case of asymmetric rectangular substitutional modulation,  $P(UVWT)$  is a trapezoidal function of  $T$  again.

The vector images discussed above are calculated for point atoms and have to be convoluted with functions considering the size and the vibrations of the atoms as well as series termination effects to get a more realistic picture. However, from Fig. 2 can be learnt that, in principle, displacive and substitutional modulation can be distinguished easily and with very good data sets (higher-order satellites), both rectangular and sinusoidal. It might even be possible to determine the extent of asymmetry of a rectangular wave.

### 3. Series termination errors

In most cases, few orders of satellite reflections are measurable only because of fluctuations of the phase, amplitude or periodicity of the modulation wave. In addition, the principal distribution of satellite intensities in reciprocal space plays an important role. For example, in the case of rectangular modulation high orders of satellites can be found around all main reflections, in principle, whereas they appear for sinusoidal modulation around highly indexed ones only. This is a consequence of the fact that the structure factor of an  $m$ th-order satellite is proportional to a trigonometric function (times  $1/m$ ) in the first case and to the  $m$ th-order Bessel function in the second one. Termination effects will therefore play an important role in the practical evaluation of the (3+1)-PF or (3+1)-FF (i.e. Fourier function). The Fourier transform of a finite set of structure factors or intensities is equal to the convolution of the true electron density or the true vector function with the Fourier transform of the (3+1)-dimensional function which gives the selection rule for the inclusion of the reflections. Thus, if we have a data set collected in the usual manner, we have a limiting sphere for the main reflections and, for the satellites, a much smaller limiting box in the extra dimension, defined by

$$f(m) = \begin{cases} 1 & \text{for } m_{\min} \leq m \leq m_{\max} \\ 0 & \text{otherwise.} \end{cases} \quad (3.1)$$

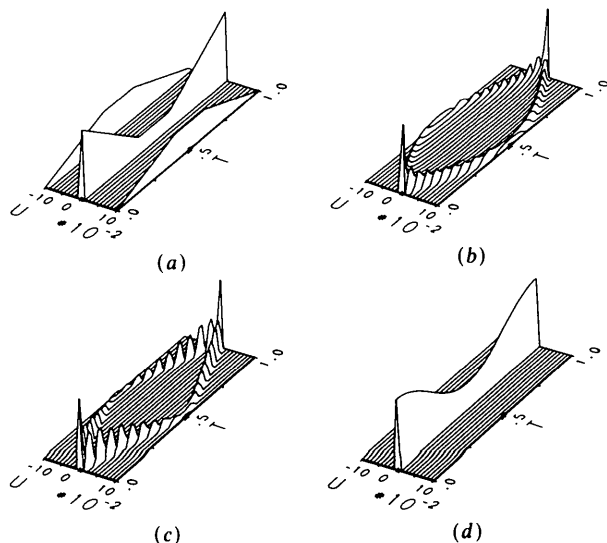


Fig. 2. The (3+1)-PF for (a) asymmetric (ratio 0.6:0.4) rectangular, (b) sinusoidal, (c) triangular displacive and (d) sinusoidal substitutional modulation. The calculations were performed for two point atoms modulated by plane waves with equal amplitudes ( $A_k^x = 0.05a$ ) and phases ( $\varphi_k^x = 0$ ). The absolute maximum is at  $\mathbf{R} = \Delta\mathbf{r}_{kk'}$  (i.e.  $U = 0$  in these plots) and  $T = \Delta\varphi_{kk'} = 0$ , the 'bordering' peaks are at  $\mathbf{R} = \Delta\mathbf{r}_{kk'} \pm (\mathbf{A}_k^x + \mathbf{A}_{k'}^x)$  (i.e.  $U = \pm 0.1$ ) and  $T = \Delta\varphi_{kk'} + \pi$  for (b) and (c). The length of the plateau parallel to the  $UT$  plane in (a) corresponds to the degree of asymmetry ( $\Delta T = 0.6 - 0.4 = 0.2$ ).

Its Fourier transform is then

$$F(T) = \int_{-\infty}^{\infty} f(m) \exp(2\pi imT) dm$$

$$= \sum_{m_{\min}}^{m_{\max}} \exp(2\pi imT). \quad (3.2)$$

If first-order satellites only have been measured we get, excluding the main reflections,

$$F(T) = 2 \cos 2\pi T. \quad (3.3)$$

If we assume phase fluctuations with a Gaussian distribution, equal for all atoms, then the limiting function can be written as  $f(m) = \exp(-n/2m^2\langle\psi^2\rangle)$  (cf. Steurer & Adlhart, 1983a) and its Fourier transform is

$$F(T) = [2\pi/(n\langle\psi^2\rangle)]^{1/2} \exp[-2\pi^2 T^2/(n\langle\psi^2\rangle)] \quad (3.4)$$

with  $n = 1$  for the (3+1)-FF and  $n = 2$  for the (3+1)-PF. Accordingly, phase fluctuations will cause a broadening of the functions along  $T$  like the Debye-Waller factor does in  $R_3$ .

Fig. 3 demonstrates the effect of series termination by convolution of the (3+1)-PF of Fig. 2(b) with (3.3). The main characteristics are not influenced thereby but the information about the shape of the modulation functions, being included in the shape of  $P(UVWT)$  as a function of  $T$ , has been lost.

In Fig. 4 an example computed with a test structure is given. In addition to series termination effects the influence of the atomic size and of thermal vibrations can be studied. The real existing structure of GeS (Bissert & Hesse, 1978) has been taken as basic structure and a sinusoidal modulation has been simulated (superspace group  $P_{111}^{Fnma}(00\gamma)$ ,  $\mathbf{q} = 0.3\mathbf{c}^*$ ,  $A_{\text{Ge}}^x = 0.02a$ ,  $A_{\text{S}}^x = 0.02a$ ,  $\varphi_{\text{Ge}} = 0$ ,  $\varphi_{\text{S}} = 0.8\lambda$ ). The (3+1)-DPF [i.e. (3+1)-dimensional difference Patterson function, calculated using satellite reflections only] of a Ge-S interaction is illustrated in Fig. 4(a). The comparison of this picture with that of Fig. 3 shows the broadening of the peaks parallel to  $U$  due to the

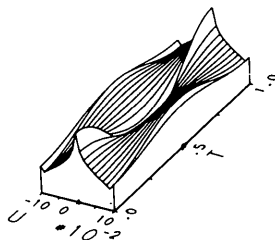


Fig. 3. The (3+1)-PF for sinusoidal modulation (cf. Fig. 2b) convoluted with equation (3.3) to simulate a Patterson synthesis calculated by the first-order satellites alone. The position of the absolute maximum ( $U = 0$ ,  $T = 0$ ) and of the 'bordering' peaks ( $U = \pm 0.1$ ,  $T = 0.5$ ) remains unaltered.

size and the thermal vibrations of the atoms involved. However, it is easy to determine the phase difference from the position of the absolute maximum at  $T = 0.8$  and the amplitudes from the 'bordering' peaks at  $T = 0.3$ .

A practical example, calculated with the intensities of the known modulated phase of  $\alpha$ -bis(*N*-methylsalicylideneaminato)nickel(II) (Steurer & Adlhart, 1983a) is represented in Fig. 5. The (3+1)-DPF for the interaction between the atoms Ni and C(8) allows a good estimation of the sum of amplitudes [ $A_{\text{Ni}}^z + A_{\text{C}(8)}^z = 0.11c$  versus 0.095 from the structure refinement] and of the phase difference [ $\Delta\varphi_{\text{Ni,C}(8)} = 0.04$  versus 0.08]. Since the superspace group of this compound  $P_{111}^{ba2}(\alpha 00)$  has symmetry elements turning

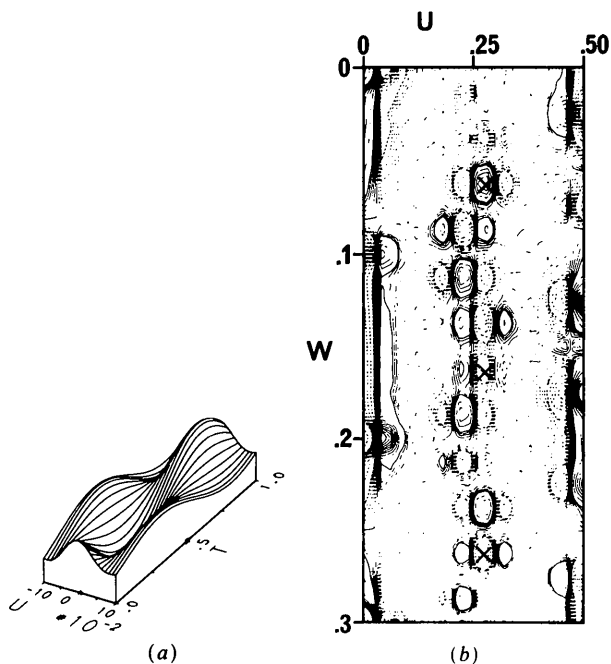


Fig. 4. (a) The (3+1)-DPF of a Ge-S interaction of the test structure calculated from the first-order satellite reflections alone. The absolute maximum is at  $U = 0$  and  $T = \Delta\varphi_{\text{Ge,S}} = 0.8$ , the 'bordering' peaks can be found at  $U = \pm 0.08a$  [corresponding to  $\mathbf{R} = \mathbf{r}_{\text{Ge,S}} \pm (A_{\text{Ge}}^x + A_{\text{S}}^x)$  on the chosen scale] and  $T = 0.3$ . (b) The 'difference Patterson synthesis' of the same structure represented in a section of the first three subcells of a tenfold superstructure ( $\pm 3\lambda$ ). The sites marked by crosses denote the Ge-S interaction used in (a).

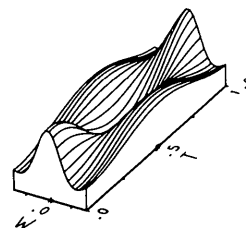


Fig. 5. The (3+1)-DPF for the interaction of the atoms Ni and C(8) of the incommensurately modulated phase of  $\alpha$ -bis(*N*-methylsalicylideneaminato)nickel(II) calculated with the first and second-order satellites. The absolute maximum is at  $W = 0$  and  $T = 0.04$ . The 'bordering' peaks are at  $W = \pm 0.11c$ .

$\mathbf{q}$  into  $-\mathbf{q}$  and the Ni atom occupies a special position with the constraint  $\varphi_{\text{Ni}} = 0$  the phase of C(8) can be determined to be  $\varphi_{\text{C}(8)} = 0.04$  or  $0.04 + \pi$ . With the same accuracy the amplitude sums and phase differences of the interactions of the Ni atom with all other non-hydrogen atoms of this structure could be derived.

The inspection of the Patterson maps of Figs. 2 to 5 shows that for average resolution no discrimination will be possible between the different shapes of modulation functions. But, in any case, displacive and substitutional modulation remain distinguishable. It is advisable to calculate the (3+1)-DPF instead of the (3+1)-PF to get a better resolution of the maximum and the 'bordering' peaks, especially, if the displacements of the modulation wave are small compared with the atomic diameters.

#### 4. General sinusoidal modulation

In this case the displacive modulation is represented by the plane waves (atom  $k$  in cell  $l$ )

$$\begin{aligned} u_{kl}^x &= A_k^x \sin 2\pi(\mathbf{q}\mathbf{r}_{kl} + \varphi_k^x), \\ u_{kl}^y &= A_k^y \sin 2\pi(\mathbf{q}\mathbf{r}_{kl} + \varphi_k^y) \\ u_{kl}^z &= A_k^z \sin 2\pi(\mathbf{q}\mathbf{r}_{kl} + \varphi_k^z) \end{aligned} \quad (4.1)$$

and the substitutional one by

$$p_{kl} = 1 + A_k^s \sin 2\pi(\mathbf{q}\mathbf{r}_{kl} + \varphi_k^s). \quad (4.2)$$

The (3+1)-PF and the (3+1)-FF can be represented by their component functions parallel to  $U$ ,  $V$  and  $W$ . These functions are calculated from the respective plane components (each one consisting of displacive and substitutional parts) alone. Thus, it might be sufficient to analyse the sections  $P(UV_0W_0T)$ ,  $P(U_0VW_0T)$  and  $P(U_0V_0WT)$  provided that the amplitudes are small compared with the atomic diameters. Otherwise, it will be necessary to study the projections of the (3+1)-PF or (3+1)-FF that one is interested in, on to the planes ( $UT$ ), ( $VT$ ), ( $WT$ ) and, to detect substitutional modulation as well as displacive, on to the line  $T$ . The bounded projection (cf. *International Tables for X-ray Crystallography*, 1959) for the limits  $U_1$ ,  $U_2$  and  $V_1$ ,  $V_2$ , for example, is

$$P_{UV}(WT) = V_c/A \int_{U_1}^{U_2} \int_{V_1}^{V_2} P(UVWT) dU dV \quad (4.3)$$

where  $A$  is the length of the unit cell in the projection. On substituting (2.1) in (4.3) and integrating twice we obtain

$$\begin{aligned} P_{UV}(WT) &= V_0/A \sum_{hklm} I_{hklm} \\ &\times [\cos 2\pi(IW + mT)(S_h S_k - C_h C_k) \\ &+ \sin 2\pi(IW + mT)(C_h S_k + S_h C_k)] \end{aligned} \quad (4.4)$$

$$\begin{aligned} C_h &= \begin{cases} 1/2\pi h(\cos 2\pi h U_2 - \cos 2\pi h U_1) & \text{for } h \neq 0 \\ 0 & \text{for } h = 0 \end{cases} \\ S_h &= \begin{cases} 1/2\pi h(\sin 2\pi h U_2 - \sin 2\pi h U_1) & \text{for } h \neq 0 \\ (U_2 - U_1) & \text{for } h = 0 \end{cases} \end{aligned}$$

and analogously for the other indices  $k$ ,  $l$ . The boundaries have to be chosen carefully to be sure that as much as possible is enclosed of the function of interest and as little as possible of the adjacent functions.

For the bounded projection on to  $T$  one has to integrate once more to obtain the expression

$$\begin{aligned} P_{UVW}(T) &= V_c \sum_{hklm} I_{hklm} \\ &\times [\cos 2\pi mT(S_h S_k S_l - S_h C_k C_l - C_h S_k C_l \\ &- C_h C_k S_l) - \sin 2\pi mT(C_h C_k C_l \\ &- C_h S_k S_l - S_h C_k S_l - S_h S_k C_l)]. \end{aligned} \quad (4.5)$$

This projection is only promising if the termination errors are negligible.

#### 5. Comparison with other Patterson methods

'Partial' or 'difference Patterson' (DPF)

The main disadvantage of this technique is that one gets information from a discrete vector function only. This results from the approximation of the incommensurate structure by a commensurate one. In the incommensurate case any site of a modulation wave will be occupied by an atom anywhere in the crystal whereas in the  $n$ -fold supercell the wave is represented by  $n$  atoms only. By analogy, the  $n$  subcells of the DPF represent  $n$  sections of the continuous (3+1)-DPF at equidistant values of  $T$ . Hence, the realizable information will be small in more complicated cases. This is illustrated in Fig. 4 where a 'difference Patterson' map of the GeS test structure is compared with the (3+1)-DPF. The Ge-S interaction vector of Fig. 4(a) is marked by crosses in the different subcells of the map. Beside the crosses the 'bordering' peaks of the (3+1)-DPF are visible. The crosses at  $W = 0.06$ ,  $0.16$  and  $0.26$  correspond to sections of the (3+1)-DPF at  $T = 0.8$ ,  $0.5$  and  $0.2$ , approximately.

'TF-Patterson' (Toman & Frueh, 1973a, b)

This method can be understood as a (3+1)-PF with heavy series termination errors computed in the fundamental cell. A Patterson map is calculated using one 'set' of satellite reflections only (order  $+m$ , for example) with the formula

$$P(\mathbf{R}) = (1/V_c) \sum_{\mathbf{H}} I_{\mathbf{H}}^{+m} \exp[-2\pi i \mathbf{R}(\mathbf{H} + m\mathbf{q})]. \quad (5.1)$$

The term

$$\begin{aligned} \mathbf{qR} &= (x\mathbf{a} + y\mathbf{b} + z\mathbf{c})(\alpha\mathbf{a}^* + \beta\mathbf{b}^* + \gamma\mathbf{c}^*) \\ &= \alpha x + \beta y + \gamma z \end{aligned} \quad (5.2)$$

corresponds to a representation of the extra dimension  $T$  in coordinates of  $R_3$ . Equation (5.1), then, can be interpreted as a partial ( $T$  is calculated for  $\mathbf{qR}$  only) (3+1)-PF convoluted with  $F(T) = \exp(2\pi imT)$ , the Fourier transform of the limiting box. The 'TF-Patterson' is a complex function and, if some preconditions are fulfilled (not too different amplitudes, for example), the maximum of the real part at  $\mathbf{R} = \Delta\mathbf{r}_{kk'}$  has the value  $\cos 2\pi(\mathbf{qR} + \Delta\varphi_{kk'})$  whereas it will be  $\sin 2\pi(\mathbf{qR} + \Delta\varphi_{kk'})$  for the imaginary one. From the ratio of both the value of  $\Delta\varphi_{kk'}$  can be evaluated.

#### 'Plus and minus DPF'

This kind of Patterson synthesis is performed in the fundamental cell or in a twofold supercell depending on the way the intensities of one satellite pair have been shrunk on the reciprocal-lattice vector  $\mathbf{H}$  or  $\mathbf{H} + \frac{1}{2}$ . The functions used thereby,

$$\begin{aligned} P^+(\mathbf{R}) &= \sum_{\mathbf{H}} (I^{+m} + I^{-m}) \cos 2\pi\mathbf{HR} \\ P^-(\mathbf{R}) &= \sum_{\mathbf{H}} (I^{+m} - I^{-m}) \sin 2\pi\mathbf{HR}, \end{aligned} \quad (5.3)$$

can be derived from the (3+1)-PF if (2.1) is written as

$$\begin{aligned} P(\mathbf{RT}) &= (1/V_c) \sum_{\mathbf{H}} \sum_{m=1}^{\infty} [(I^{+m} + I^{-m}) \\ &\quad \times \cos 2\pi\mathbf{HR} \cos 2\pi mT \\ &\quad - (I^{+m} - I^{-m}) \sin 2\pi\mathbf{HR} \sin 2\pi mT] \end{aligned} \quad (5.4)$$

(excluding the main reflections). Setting  $T=0$ , one obtains  $P^+$  and, for  $T=3\pi/2$ ,  $P^-$  results. The 'plus and minus DPF' corresponds to sections of the (3+1)-DPF, therefore. Similar information can be obtained as in the case of the 'TF-Patterson'.

### 6. The application of the (3+1)-dimensional Fourier function

The (3+1)-FF was first studied by Yamamoto (1982) but has not been used as an aid for the solution of modulated structures until now. It can be calculated by the formula

$$\begin{aligned} \rho(XYZT) &= 1/V_c \sum_h \sum_k \sum_l \sum_m F_{hklm} \\ &\quad \times \exp[-2\pi i(hX + kY + lZ + mT)]. \end{aligned} \quad (6.1)$$

The (3+1)-FF and the (3+1)-DFF [difference

Fourier function with  $(F_{hklm}^{\text{obs}} - F_{hklm}^{\text{calc}})$  as Fourier coefficients] can similarly be used in the course of the refinement of the modulated structure as their three-dimensional analogues in conventional structure analysis. Incorrectly calculated modulation parameters could be detected in this way, and calculation effects could be distinguished from real structural properties, for example, whether the modulation is a plane wave (with  $\varphi_x = \varphi_y = \varphi_z$ ) or not.

Another possibility provided that higher-order satellites are included is finding indications to the existence of fluctuations of the phase or the amplitude of the modulation wave (cf. Adlhart, 1982) if they are of the order of the Debye-Waller factor.

Both the fluctuations cause a spatially modulated contribution to the modulation (with a wave vector  $2\mathbf{q}$ ) which has a phase shift of  $\pi/2$  in the case of phase fluctuation. Thus, in this case, the (3+1)-DFF would show positive regions along  $T$  around the nodal points, whereas in the case of amplitude fluctuations the positive difference density could be found around both the extremal values with a distribution parallel to  $\mathbf{A}_k$ .

If one finds positive and negative regions parallel to  $\mathbf{A}_k$  separated by  $\pi$  from each other it could be caused by the first harmonic of the modulated temperature factor (cf. Yamamoto, 1982).

### 7. Concluding remarks

Following the determination of the average structure, the assignment of the superspace group (cf. de Wolff, Janssen & Janner, 1981) and the qualitative analysis of the diffraction pattern (cf. Jagodzinski, 1984), the (3+1)-PF can be very helpful for the evaluation of starting parameters for the structure refinement. It will be promising in all cases showing well resolved peaks in the Patterson maps of the average structure. In the initial stages of the refinements the (3+1)-FF and (3+1)-DFF can be a valuable aid to obtain the modulation parameters for the atoms which have not been considered by the Patterson syntheses and, in general, to control the results of the refinements as in the classical structure analysis. A structure determination of the modulated structure of an andesine  $\text{An}_{38}$  has been performed successfully using the methods mentioned above (Steurer & Jagodzinski, 1986).

#### References

- ADLHART, W. (1982). *Acta Cryst.* **A38**, 498-504.  
 BISSERT, G. & HESSE, K. F. (1978). *Acta Cryst.* **B34**, 1322-1323.  
 BÖHM, H. (1978). *Z. Kristallogr.* **148**, 207-220.  
 BÖHME, R. (1982). *Acta Cryst.* **A38**, 318-326.  
 FRUEH, A. J. (1953). *Acta Cryst.* **6**, 454-456.  
 HORST, W., TAGAI, T., KOREKAWA, M. & JAGODZINSKI, H. (1981). *Z. Kristallogr.* **157**, 233-250.  
*International Tables for X-ray Crystallography* (1959). Vol. II. Birmingham: Kynoch Press. (Present distributor D. Reidel, Dordrecht.)

- JAGODZINSKI, H. (1984). *Bull. Minéral.* **107**, 455-466.  
 MCCONNELL, J. D. C. & HEINE, V. (1984). *Acta Cryst.* **A40**, 473-482.  
 STEURER, W. & ADLHART, W. (1983a). *Acta Cryst.* **B39**, 349-355.  
 STEURER, W. & ADLHART, W. (1983b). *Acta Cryst.* **B39**, 721-724.  
 STEURER, W. & JAGODZINSKI, H. (1986). In preparation.  
 TAKÉUCHI, Y. (1972). *Z. Kristallogr.* **135**, 120-136.  
 TOMAN, K. & FRUEH, A. J. (1973a). *Acta Cryst.* **A29**, 121-127.  
 TOMAN, K. & FRUEH, A. J. (1973b). *Acta Cryst.* **A29**, 127-133.  
 TOMEOKA, K. & OHMASA, M. (1982). *Am. Mineral.* **67**, 360-372.  
 WOLFF, P. M. DE (1974). *Acta Cryst.* **A30**, 777-785.  
 WOLFF, P. M. DE, JANSSEN, T. & JANNER, A. (1981). *Acta Cryst.* **A37**, 625-636.  
 YAMAMOTO, A. (1982). *Acta Cryst.* **A38**, 87-92.  
 YAMAMOTO, A., NAKAZAWA, H., KITAMURA, M. & MORIMOTO, N. (1984). *Acta Cryst.* **B40**, 228-237.

*Acta Cryst.* (1987). **A43**, 42-44

## Atomic Scattering Factors for Mixed Atom Sites

BY KEITH D. SALES

*Department of Chemistry, Queen Mary College, Mile End Road, London E1 4NS, England*

(Received 23 April 1986; accepted 21 May 1986)

### Abstract

A method is presented for the calculation of analytical coefficients for scattering factors at mixed atom sites. The importance of the concept of compatible coefficients for the separate atoms is stressed and examples of the problems that can arise when trying to find coefficients for mixed atom sites are given. A computer program and its use are described. Two errors in *International Tables for X-ray Crystallography* [(1974). Vol. IV. Birmingham: Kynoch Press. (Present distributor D. Reidel, Dordrecht)] are noted, for  $\text{Ru}^{4+}$  and  $\text{Bi}^{5+}$ , for which revised coefficients are given. For  $\text{N}$ ,  $\text{O}^-$  and  $\text{Sr}^{2+}$  analytical coefficients are given which fit the tabulated scattering factors significantly better than the coefficients in *International Tables for X-ray Crystallography*.

### 1. Introduction

The atomic scattering factor is used to describe the coherent scattering of X-rays by an atom. It is a function of the electron density of the atom and the finite size of this density causes the scattering factor to depend upon the Bragg angle  $\theta$  and the wavelength of the X-rays  $\lambda$  through the parameter  $x = \sin\theta/\lambda$ . The electron density of an atom is known only by theoretical calculation so the scattering factor is approximate and depends upon the reliability of the theory; various calculations have been used and the resulting factors tabulated for a range of  $x$  values between 0 and 2 (*International Tables for X-ray Crystallography*, 1974, pp. 82-98).

Tables of such values were used in older X-ray computer programs, scattering factors for non-tabulated  $x$  values being obtained by linear interpolation. More recent programs use an analytical expression

of the form:

$$f_c(x) = \sum_{i=1}^4 a_i \exp[-b_i x^2] + c, \quad (1)$$

with values of  $\mathbf{a}$  ( $= a_i, i = 1$  to 4),  $\mathbf{b}$  ( $= b_i, i = 1$  to 4) and  $c$  being tabulated for different atoms (*International Tables for X-ray Crystallography*, 1974, pp. 99-101). The  $\mathbf{a}$ ,  $\mathbf{b}$  and  $c$  for a particular atom are obtained by minimizing the difference between  $f_c(x)$ , the value calculated from such an expression, and  $f(x)$ , the tabulated value. The statistic used here to obtain this best fit is

$$\chi^2 = \sum_{i=1}^n [f(x_i) - f_c(x_i)]^2 / (n - 9),$$

where  $n$  is the number of  $x$  values used in the fitting, those used here being  $x_i = 0.0$  (0.01) 0.20 (0.02) 0.50, 0.55, 0.60, 0.65, 0.70 (0.10) 2.00, a maximum of 53 values, although for some cases  $f(x)$  is quoted for only the first 48 values.

Some structures contain a mixture of two different atoms occupying the same type of site as, for instance, NO and CO groups or  $\text{Na}^+$  and  $\text{K}^+$  ions disordered in a lattice. In these cases an average scattering factor has to be used:

$$f(x) = x_A f_A(x) + x_B f_B(x), \quad (2)$$

where  $x_A$  is the mole fraction of atom  $A$  with scattering factor  $f_A$  and similarly for  $B$ . With tabulated values of  $f_A$  and  $f_B$  this averaging is trivial, but with the analytical expression for  $f$  there is a complication in existing computer programs which require coefficients for each 'atom', regardless of whether that 'atom' is a mixture of two atoms or not. Thus the problem is to express  $x_A f_A(x) + x_B f_B(x)$  in the form of (1).